

Journal of Materials Chemistry B

Accepted Manuscript



This is an *Accepted Manuscript*, which has been through the Royal Society of Chemistry peer review process and has been accepted for publication.

Accepted Manuscripts are published online shortly after acceptance, before technical editing, formatting and proof reading. Using this free service, authors can make their results available to the community, in citable form, before we publish the edited article. We will replace this *Accepted Manuscript* with the edited and formatted *Advance Article* as soon as it is available.

You can find more information about *Accepted Manuscripts* in the [Information for Authors](#).

Please note that technical editing may introduce minor changes to the text and/or graphics, which may alter content. The journal's standard [Terms & Conditions](#) and the [Ethical guidelines](#) still apply. In no event shall the Royal Society of Chemistry be held responsible for any errors or omissions in this *Accepted Manuscript* or any consequences arising from the use of any information it contains.

ARTICLE

Detection of human immunoglobulin G by label-free electrochemical immunoassay modified with ultralong CuS nanowires

Cite this: DOI: 10.1039/x0xx00000x

Received 00th November 2014,
Accepted 00th November 2014

DOI: 10.1039/x0xx00000x

www.rsc.org/

Ning Wang^a, Caizhen Gao^{a, b}, Yu Han^{a, b}, Xiaomin Huang^{a, b}, Ying Xu^{a, b}, and Xia Cao^{b, c*}

Ultralong copper sulfide nanowires (CuSNWs) were synthesized via a simple wet chemical route. Due to the desired surface charge characteristics and attractive electrocatalytic activity toward the oxidation of ascorbic acid, such ultralong one-dimensional nanomaterials provided an interesting platform for electrochemical signal amplification. By immobilizing anti-IgG antibody on the chitosan (CS)-CuSNWs film, a novel label-free electrochemical immunosensor was thus developed for detection of human immunoglobulin G (IgG). Various experimental parameters were studied, and the interference effects from other proteins were checked. Under the optimum condition, the decrease of amperometric signal presented a linear relationship in the IgG concentration range of 0.001-320 ng/mL with a detection limit of 0.1 pg/mL (S/N=3). Practical application of the fabricated immunosensor has also been demonstrated by detecting IgG in real human serum samples. The satisfactory results hint the significant potential in clinical analysis.

1. Introduction

Accurate and sensitive detection of proteins is of great importance in both biomedical researches and clinical diagnosis.¹⁻⁴ Various immunoassay methods such as fluorescence⁵, chemiluminescence⁶, surface plasmon⁷, and mass spectrometric immunoassays^{8, 9} have been developed for the detection of different proteins.¹⁰⁻¹² However, these methods often suffer from considerable time consumption, high cost and tediously professional operation, which make them less appropriate for practical applications and call a more convenient detection method with a comparable or even higher sensitivity.^{13, 14} In this sense, the electrochemical label-free immunoassay is ideal for detection of proteins and has recently aroused extensive interest due to its rapid recognition, simple instrumentation and easy operation.¹⁵⁻¹⁹

Recent progress in nanoscience offers bountiful opportunities for the rational design of functional materials with unique surface and electronic properties for electrochemical immunoassay.²⁰⁻²² The large surface-to-volume ratio of nanomaterials ensures the immobilization of a sufficient amount of recognition elements, while the high electronic conductivity, excellent catalytic activity and biocompatibility provide significantly improved signal transductions.²³⁻²⁷ As a result, high sensitivity, good selectivity, low detection limit, fast response, and miniaturization of the sensing devices can be achieved.²⁸⁻³¹

As an important p-type semiconductor, copper sulfide (CuS) has been extensively used for wide applications including high-capacity cathode material, nanometer-scale switches, photo catalyst and optical sensor.³²⁻³⁵ In the last few years, motivated

by the so-called size- and structure-dependent properties, nanoscale CuS such as nanospheres, nanowires, nanoplates, hollow spheres, nanotubes, and nanorods have been synthesized.^{34, 36-39} All the same, reports on the applications in the area of electrocatalysis or electrochemical sensing are rather rare in comparison with the vast quantity of reports on CuS used for optics.⁴⁰⁻⁴²

In this paper, CuS nanowires were synthesized by a facile water solution-based route and then used to develop a highly sensitive label-free electrochemical immunosensor. Due to the sound electrocatalytic activity toward the oxidation of AA, the as-proposed sensor shows great potential for the detection of human IgG. Various experimental parameters affecting the IgG detection were optimized and the detection limit was determined. Possible practical applications of the IgG immunosensor were discussed and examined in real human serum samples. The sound acceptable selectivity, stability as well as reproducibility make the as-prepared CuS nanowires very promising for practical clinical purposes.

2. Experimental

2.1 Reagents.

Human IgG (IgG), anti-IgG, human serum albumin (HSA), bovine serum albumin (BSA), thrombin (TB), alpha-fetoprotein (AFP) and carcino embryonic antigen (CEA) were purchased from Sigma (USA). Ascorbic acid (AA), chitosan (CS), copper chloride ($\text{CuCl}_2 \cdot 2\text{H}_2\text{O}$), D-glucose ($\text{C}_6\text{H}_{12}\text{O}_6 \cdot 3\text{H}_2\text{O}$), and hexadecylamine ($\text{C}_{16}\text{H}_{35}\text{N}$) were obtained from Sigma-Aldrich Chemical Company (St. Louis, MO). All other reagents, unless otherwise noted, were of analytical grade and were used without further purification. Phosphate-buffered solution (PBS, 0.1 M, pH 7.4) was prepared and used as a working solution. A blocking buffer was prepared by dissolving 2% (w/v) BSA in PBS. Clinical human serum samples were provided by the Third Hospital of Peking University and used as received. Ultrapure water obtained from a Millipore water purification system was used throughout the experiments.

2.2 Synthesis of CuS nanowires.

In a typical synthesis, 0.1 g of copper chloride, 0.7 g of hexadecylamine and 0.2 g of glucose were dissolved in 50 mL of pure water under vigorous stirring. The mixture was placed in a Teflon-lined stainless steel autoclave of 100 mL capacity and kept first at 60 °C for 4 h and then 120 °C for another 3 h. After harvested with centrifugation-redispersion cycles with deionized water and ethanol for 6 times, the final copper sulfide products were obtained by hydrothermally treating the above copper with 50 mL of 0.2 M of Na_2S solution at 120 °C for 2 h.

2.3 Preparation of electrochemical immunosensors.

Schematic illustration of the stepwise procedure for the preparation of the immunosensor is displayed in Fig. 1. In this scheme, CuSNWs are used as signal transducers and coupled with CS to form the nanocomposite film on a glassy carbon

electrode (GCE). Enhanced signal amplification is expected from the demonstrated catalytic activity of the one-dimensional CuS nanomaterials toward the oxidation of AA. The antibody of IgG (anti-IgG) is employed as a model for conjugating to the nanocomposite film via the strong physical and electrostatic adsorptions. When the reaction between anti-IgG and IgG occurs, the electrocatalytic response to AA dramatically decreases owing to the production of weakly conductive immunocomplex layer.

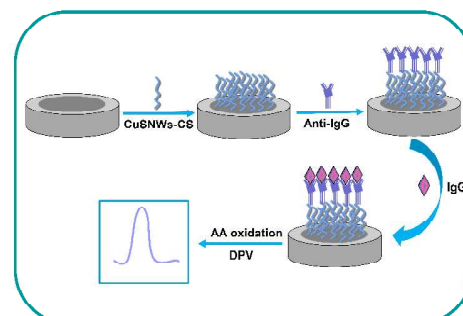


Fig. 1 Schematic routine of the label-free electrochemical immunosensing platform for IgG.

To fabricate the electrochemical immunosensors, a glassy carbon electrode (GCE, 3 mm in diameter, Shanghai, CHI Instrument Co.) was polished with 0.05 μM alumina/water slurry on a polishing cloth to a mirror finish, followed by sonicating and rinsing with distilled water. 7 μL of CuSNWs/CS (5 mg of CuSNWs dispersed in 5 mL of 1 wt% CS solution) was then dipped onto the GCE electrode surface. After dried in air, anti-IgG solution (100 $\mu\text{g}/\text{mL}$) was immediately dropped onto the electrode surface and incubated for 2 h to form an anti-IgG/CuSNWE electrode at room temperature. The modified GCE was then rinsed thoroughly with the 0.1 M PBS to remove the weakly adsorbed anti-IgG and subsequently blocked by incubating for 1.0 h in a 2% BSA solution for minimizing the non-specific binding. Subsequently, the electrode was then incubated for 35.0 min in a PBS solution containing human IgG at various concentrations. After washing, the desired immunosensor was finally obtained and stored at 4 °C in a dry environment prior to use.

2.4 Characterization techniques.

Morphological information of the as-synthesized CuS nanowires was characterized by using a Hitachi S4800 cold field emission scanning electron microscope (CFE-SEM) and a JOEL 2100F transmission electron microscopy (TEM). The X-ray powder diffraction (XRD) pattern of the products was collected using a Rigaku X-ray diffractometer (Rigaku Goniometer PMG-A2, CN2155D2, wavelength = 0.15147 nm) with Cu $K\alpha$ radiation. Differential pulse voltammetry (DPV) was performed at room temperature under PBS (pH = 7.4) solution on a CHI 660C electrochemical station, using a single compartment and three electrode cell. GCE was used as working electrode, while saturated calomel electrode (SCE) was used as reference electrode and a Pt wire as counter

electrode. The data of conditions, optimization and practicability were the average of five measurements.

3. Results and discussion

3.1 Characterization of CuS nanowires.

Figure 2A shows SEM image of CuS nanowires. The products consisted of uniform nanowires with an average length of 70 micrometers and diameter of 30 to 50 nm. Lattice resolved TEM images (Figs. 2B-C) revealed the sound crystallinity and $\langle 0001 \rangle$ growth orientation. XRD pattern (Fig. 2D) demonstrated the nanowire had a hexagonal structure. The one-dimensional nanostructure was sufficiently stable and remained unchanged even after long-time rinse and ultrasonication both in water and organic solvents (Fig. S1).

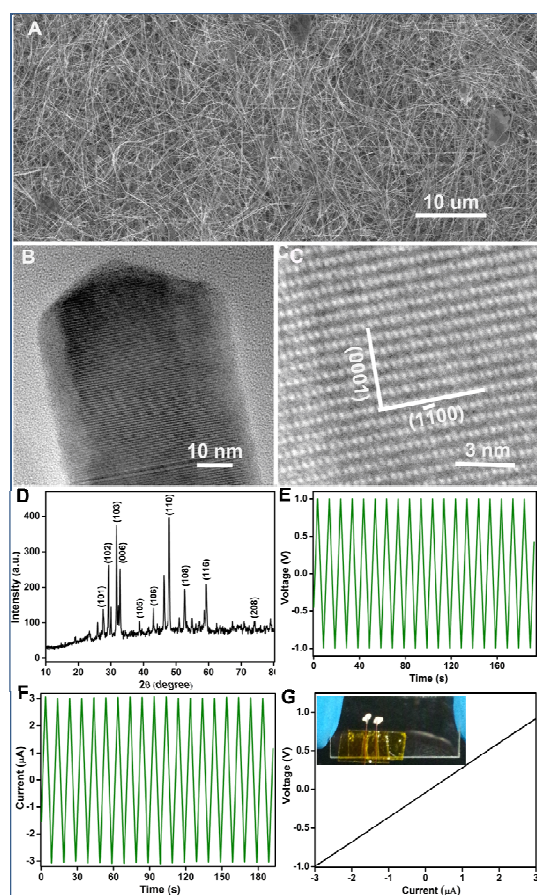


Fig. 2 Typical information of the CuS nanowires: (A) SEM image; (B-C) TEM and HRTEM images at different magnifications; (D) XRD pattern; (E-G) The resistance of CuS nanowire measured by the synthesized function generator and a low noise current amplifier.

For electrochemical sensing, the resistance of CuS nanowire is important for signal amplification, which was thus measured by the synthesized function generator (Stanford Research Systems DS345) and a low noise current amplifier (Stanford Research Systems SR570) (see Figs. 2E-G). The relatively low resistance may be ascribed to the typical 1D nanostructure and deserved further study, which provides accesses to not only semiconductor superiority (specific biocompatibility and high

electrocatalytic activity), but also the nanowire structural superiority (high specific area and enhanced electron transfer rate). For these reasons, the ultralong CuS nanowires are sound candidates for catalysis-based applications. The three-dimensional network of interconnected CuS nanowires provide an enhanced beam transmission as well as scattering of free electrons, thus contributes to the high electron transfer rate.⁴³

3.2 Characterization of immunosensor array.

Due to the excellent film forming ability and abundant amino-groups, CS was used for functionalizing CuS nanowires. A well-dispersed homogeneous suspension of CuSNWs-CS composite was dropped onto the working electrode to fabricate a porous CuSNWs-CS film (Fig. 3A). Aggregations of anti-IgG molecules were then trapped onto the nanowire surface by incubating the electrode in anti-IgG solution (100 $\mu\text{g}/\text{mL}$) for 2 hours (Fig. 3B). In this strategy, the amino groups in CS provide a hydrophilic environment compatible with the biomolecules. The interconnected CuSNWs are expected to increase the contact points for good electrical connection and eliminate the randomization of electron transportation in the immunosensor array.

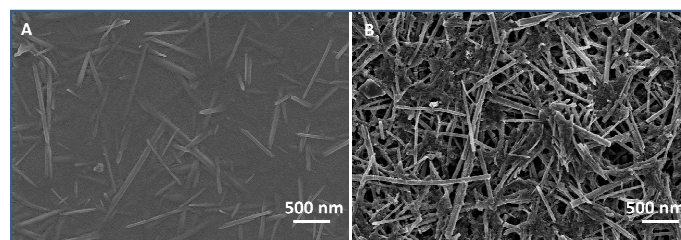


Fig. 3 Typical SEM images of CuSNWs-CS (A), and anti-IgG/CuSNWs-CS (B).

3.3 Electrochemical behavior of immunosensor.

Here a label-free electrochemical immunosensor for detection of IgG was developed on the base of the detection of the current signal at the CuSNWE electrode. Differential pulse voltammetry (DPV) curves were recorded to interrogate the changes of the electrode behaviour after each assembly step in a pH 7.4 PBS solution. As shown in Fig. 4A, a weak peak was observed on bare GCE electrode in pH 7.4 PBS solution contained 5 mM AA. However, a well-defined DPV peak at 0.01 V can be seen on the CuSNWE electrode (curve B, Fig. 4). This result turned out that CuS NWs are essential in the electrochemical measurement. When anti-IgG was immobilized onto the CuSNWE electrode surface, the peak currents of oxidation decreased (Fig. 4, curve C). A further decrease in the amperometric response was observed on the IgG/anti-IgG/CuSNWE electrode after anti-IgG antibody molecules combined with the antigen molecules (curve D, Fig. 4). It is well known that formation of immunocomplex can result in the decrease of detection signal in electrochemical immunoanalysis. Because adsorption of large biomolecules at the electrode surface, the interfacial capacitance will change.⁴⁴ So, the detection of IgG can be obtained from the change of the

oxidation peak amperometric response before and after the antigen-antibody reaction.

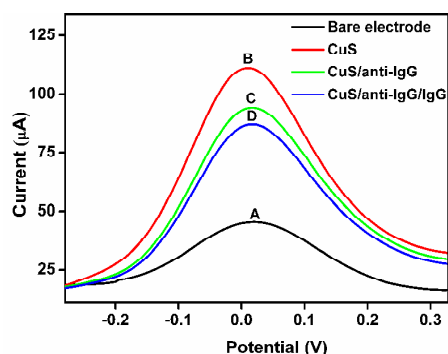


Fig. 4 DPV responses of different electrodes in pH 7.4 PBS solution containing 5 mM AA, (A) bare GCE electrode, (B) CuSNWE electrode, (C) anti-IgG/CuSNWE electrode, (D) IgG/anti-IgG/CuSNWE electrode.

3.4 Optimization of the immunoassay procedure.

The experimental parameters such as anti-IgG concentration, IgG incubation time, pH of the detection solution, and the effect of temperature were optimized for the detection of IgG. Several CuSNWE electrodes bearing different amounts of antibody were fabricated and tested for different concentrations of target analyte, IgG. It can be seen that the maximum slope was obtained at 100 $\mu\text{g}/\text{mL}$ anti-IgG, suggesting that the highest sensitivity for IgG detection can be achieved at this condition. Hence, 100 $\mu\text{g}/\text{mL}$ of anti-IgG was thus selected as the optimal concentration (Fig. 5A). Figure 5B shows the pH effect of the detection solution in the pH range of 5.5 - 9. The current change increased with the increase of pH value from 5.5 and then decreased from 7.4. The decrease in the current variation over pH 7.4 can be ascribed to the weak immuno-interaction at higher pH.⁴⁵ The optimum pH was fixed to be 7.4 because here the optimal amperometric response could be observed. Figures 5C-D depict the relationship of ΔI with the incubation temperature and time. A slight increase of the amperometric response was first observed along with the increase of incubation temperature, which reached a plateau at 37°C. Thus the analytical process can be simplified by carrying out all the experiments at room temperature. This simplification will not make any significant difference on the final results in comparison with that at 37°C. Furthermore, the amperometric response of the immunoassay increased from 10.0 min, and reached a maximum at 35.0 min of incubation time. Therefore, 35 min of incubation time was fixed for the determination of IgG antigen in this study.

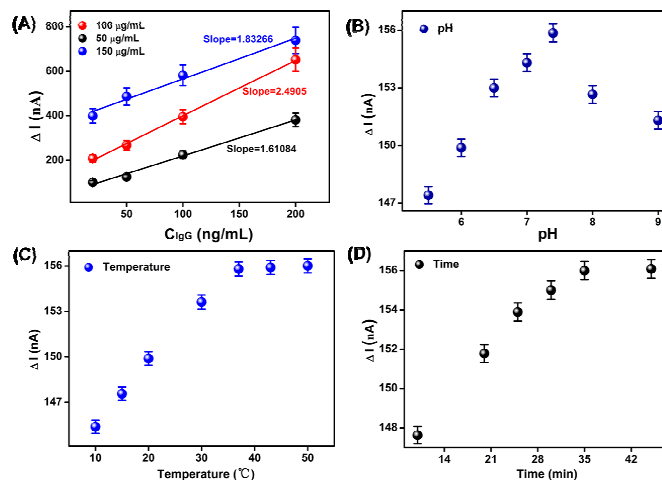


Fig. 5 Optimization of experimental conditions including (A) anti-IgG concentration, (B) pH effect of detection solution, (C) incubation temperature and (D) incubation time on peak current responses of the immunosensor toward 10 ng/mL IgG.

3.5 Analytical performance of the immunosensor.

The sensitivity and dynamic range of the electrochemical immunosensor were determined by measuring the DPV responses of the CuSNW-based label free immunosensor using AA as electrochemical substrate under optimal conditions. As expected, a decrease of the peak currents of the immunosensor for IgG measurement can be observed along with the increase of concentration of analyte after the antigen-antibody reaction (Fig. 6A). The calibration plot in Fig. 6B showed a linear relationship between the change of peak currents and the concentrations of IgG in the range from 0.001 to 320 ng/mL. Based on $S/N = 3$, a detection limit of 0.1 $\mu\text{g}/\text{mL}$ could be obtained (Fig. S2), which is comparable with, if not lower than, that of the previous reports (Table 1). The excellent electrochemical performance can be attributed to the very high aspect ratio, sound conductivity, large specific surface, and well-dispersion of CuSNWs, which effectively increases the electrocatalytic active areas and promotes electron transfer in the oxidation of AA.

Table 1 Performance comparison of the proposal methods for IgG

Method	Linear range (ng/mL)	Detection limit (ng/mL)	Reference
stripping voltammetry	0.001-100	0.0004	46
electrochemical immunosensor	7.5×10^{-5} - 1.44×10^8	1.2×10^5	47
electrochemical measurement	0.02-500	0.0097	48
sandwich-type immunoassay	1.5-2250	0.75	49
quartz crystal microbalance	0-2500	46	50

sandwich-type immunoassay	0.01-200	0.004	51
label-free immunoassay	0.001-320	0.0001	this work

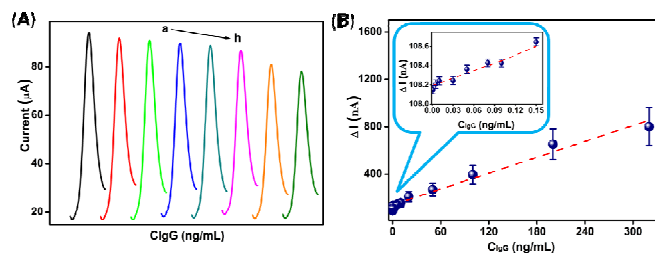


Fig. 6 DPV responses of the proposed immunosensor toward different concentrations of IgG (0.1, 0.5, 1, 5, 10, 20, 50, 100, 200, 320 ng/mL) (A); Calibration curve using the developed immunosensor (B), the inset shows the calibration curve at lower IgG concentrations (0.001, 0.005, 0.01, 0.03, 0.05, 0.08, 0.1, 0.15 ng/mL).

3.6 Selectivity, reproducibility and stability of the immunosensor.

The selectivity of the immunosensor was tested by carrying out comparative experiments between IgG and other interfering proteins under the same condition. In this comparison, bovine serum albumin (BSA), human serum albumin (HSA), thrombin (TB), alpha-fetoprotein (AFP) and carcino embryonic antigen (CEA) were selected and the current responses were measured, respectively. As depicted in Fig. 7, none of the 300 ng/mL interfering proteins caused any obvious current signal change (closed to the background), while 100 ng/mL IgG led to an obvious variation of current signal. Additionally, four parallel experiments demonstrated the proposed biosensor presented sound selectivity for discrimination of IgG from other proteins.

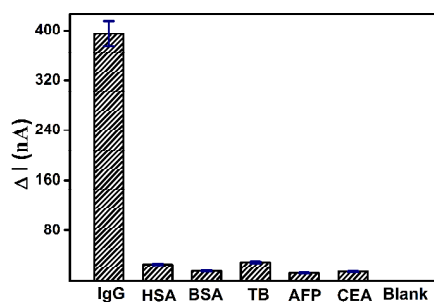


Fig. 7 Detection selectivity of the proposed immunosensor toward 100 ng/mL IgG by comparing it to other interfering proteins (300 ng/mL): HSA, BSA, TB, AFP and CEA and blank control. Error bar = RSD (n = 4).

Five immunosensors were parallelly prepared for the repeated measurements of the same concentrations of IgG (50 ng/mL). The five immunosensors, though made independently, showed the current responses of 82.4, 81.3, 87.5, 89.6, 88.1 μ A. The reproducibility expressed in terms of the relative standard deviation (RSD) was about 4.3%. These results indicated that the immunosensor possessed sound reproducibility.

In addition, the stability of the CuSNWs-based immunosensor was also studied by measuring the current response after stored for five weeks in dry condition at 4 °C. The resulting signal had no significant difference with the fresh prepared one (Fig. 8). This indicates that the sensor also owns the good stability, which can be partly attributed to the firmly bonding of antibody to the electrode surface.

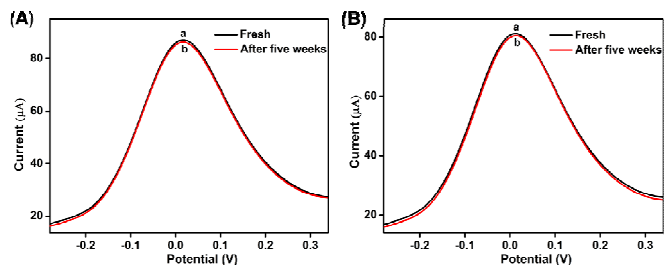


Fig. 8 The stability of the developed immunosensor to IgG: (A) 100 ng/mL IgG, (B) 200 ng/mL IgG. Black solid lines represent the fresh one, red solid lines represent the one after stored for five weeks.

3.7 Applications of the immunosensor.

In order to examine the practicability of the designed sensor for real sample assay, recovery experiments were also performed by the standard addition method. Different concentrations of IgG (1.0, 10, 50, 100 ng/mL) were added into human serum samples, respectively and were analyzed by the immunosensing method. The test results indicated that the IgG recovery was between 99.7% and 101.2% with RSD values ranging from 2.03% to 4.13% (Table 2). This is an acceptable reliability for practical applications.

Table 2 Recovery tests of IgG in human serum sample

No.	added (ng/mL)	Found (ng/mL)	RSD (%)	Recovery (%)
1	1.0	1.04, 1.05,	4.13	100.6
		1.01, 0.95,		
		0.98		
2	10.0	10.32, 10.26,	2.63	100.6
		9.75, 10.18,		
		9.81		
3	50.0	51.25, 50.43,	2.37	99.7
		50.32, 49.09,		
		48.27		
4	100.0	101.34, 102.78,	2.03	101.2
		103.58, 99.60,		
		98.72		

4. Conclusions

In summary, a label-free electrochemical immunosensor for the ultrasensitive detection of IgG has been successfully designed by utilizing the ultralong CuS nanowires as novel signal amplifier. Due to relative low resistance, high specific surface areas, faster electron transfer and uncommon catalytic activity of CuSNWs toward AA oxidation, the proposed immunosensor exhibited a wide linear range, low detection

limit, good selectivity, satisfactory stability and acceptable practicability for the detection of antigen. Therefore, this method provides a promising strategy for protein biomarker determination in clinical application.

Acknowledgements

We thank the financial support from the National Natural Science Foundation of China (NSFC No. 21275102, 21173017, and 21075004), the Program for New Century Excellent Talents in University (NCET-12-0610), the science and technology research projects from education ministry (213002A), National "Twelfth Five-Year" Plan for Science & Technology Support (No. 2013BAK12B06), and the "thousands talents" program for pioneer researcher and his innovation team, China.

Notes and references

^a School of Chemistry and Environment, Beijing University of Aeronautics and Astronautics, Beijing, 100191, China.

^b Beijing Institute of Nanoenergy and Nanosystems Chinese Academy of Science, Beijing, 100083, China.

^c School of Chemistry and Biological Engineering, University of Science and Technology Beijing, Beijing, 100083, China.

* To whom all correspondence should be addressed. E-mail: caoxia@binn.cas.cn (X.C.).

- Y. Chen, E. R. Cruz-Chu, J. C. Woodard, M. R. Gartia, K. Schulten and L. Liu, *Acs Nano*, 2012, 6, 8847-8856.
- A. Hucknall, S. Rangarajan and A. Chilkoti, *Adv Mater*, 2009, 21, 2441-2446.
- D. Khatayevich, T. Page, C. Gresswell, Y. Hayamizu, W. Grady and M. Sarikaya, *Small*, 2014, 10, 1505-1513.
- P. W. Yen, C. W. Huang, Y. J. Huang, M. C. Chen, H. H. Liao, S. S. Lu and C. T. Lin, *Biosens Bioelectron*, 2014, 61, 112-118.
- Q. L. Yu, X. Wang and Y. X. Duan, *Anal Chem*, 2014, 86, 1518-1524.
- F. Ma, Y. Yang and C. Y. Zhang, *Anal Chem*, 2014, 86, 6006-6011.
- J. S. Lane, J. L. Richens, K. A. Vere and P. O'Shea, *Langmuir*, 2014, 30, 9457-9465.
- A. Nazabal, R. J. Wenzel and R. Zenobi, *Anal Chem*, 2006, 78, 3562-3570.
- K. Meyer and P. M. Ueland, *Anal Chem*, 2014, 86, 5807-5814.
- J. S. Lee, H. A. Joung, M. G. Kim and C. B. Park, *Acs Nano*, 2012, 6, 2978-2983.
- T. Li, E. J. Jo and M. G. Kim, *Chem Commun*, 2012, 48, 2304-2306.
- C. Xie, F. G. Xu, X. Y. Huang, C. Q. Dong and J. C. Ren, *J Am Chem Soc*, 2009, 131, 12763-12770.
- S. J. Lehotay and R. W. Miller, *J Environ Sci Heal B*, 1994, 29, 395-414.
- H. C. Guo and S. Q. Sun, *Nanoscale*, 2012, 4, 6692-6706.
- J. Zhou, M. D. Xu, D. P. Tang, Z. Q. Gao, J. Tang and G. N. Chen, *Chem Commun*, 2012, 48, 12207-12209.
- L. Yang, H. Zhao, S. M. Fan, S. S. Deng, Q. Lv, J. Lin and C. P. Li, *Biosens Bioelectron*, 2014, 57, 199-206.
- X. Cao, Y. Han, C. Z. Gao, X. M. Huang, Y. Xu and N. Wang, *J Mater Chem A*, 2013, 1, 14904-14909.
- K. V. Singh, D. K. Bhura, G. Nandamuri, A. M. Whited, D. Evans, J. King and R. Solanki, *Langmuir*, 2011, 27, 13931-13939.
- J. Du, Q. F. Xu, X. Q. Lu and C. Y. Zhang, *Anal Chem*, 2014, 86, 8481-8488.
- S. K. Mishra, A. K. Srivastava, D. Kumar, A. M. Biradar and Rajesh, *Nanoscale*, 2013, 5, 10494-10503.
- J. F. Rusling, G. W. Bishop, N. M. Doan and F. Papadimitrakopoulos, *J Mater Chem B*, 2014, 2, 12-30.
- X. Q. Lu, Y. Li, X. Zhang, J. Du, X. B. Zhou, Z. H. Xue and X. H. Liu, *Anal Chim Acta*, 2012, 711, 40-45.
- B. A. Legg, M. Q. Zhu, L. R. Comolli, B. Gilbert and J. F. Banfield, *Langmuir*, 2014, 30, 9931-9940.
- Z. Ren and P. X. Gao, *Nanoscale*, 2014, 6, 9366-9400.
- H. G. Liao, D. Zherebetsky, H. L. Xin, C. Czarnik, P. Ercius, H. Elmlund, M. Pan, L. W. Wang and H. M. Zheng, *Science*, 2014, 345, 916-919.
- X. Cao, N. Wang, S. Jia and Y. H. Shao, *Anal Chem*, 2013, 85, 5040-5046.
- J. J. Zhang, J. L. Wang, J. J. Zhu, J. J. Xu, H. Y. Chen and D. K. Xu, *Microchim Acta*, 2008, 163, 63-70.
- S. X. Wu, Q. Y. He, C. L. Tan, Y. D. Wang and H. Zhang, *Small*, 2013, 9, 1160-1172.
- S. J. Guo and E. K. Wang, *Nano Today*, 2011, 6, 240-264.
- S. J. Guo and S. J. Dong, *J Mater Chem*, 2011, 21, 16704-16716.
- J. J. Zhang and J. J. Zhu, *Sci China Ser B*, 2009, 52, 815-820.
- J. S. Chung and H. J. Sohn, *J Power Sources*, 2002, 108, 226-231.
- J. R. Huang, Y. Y. Wang, C. P. Gu and M. H. Zhai, *Mater Lett*, 2013, 99, 31-34.
- J. Liu and D. F. Xue, *J Mater Chem*, 2011, 21, 223-228.
- X. M. Qian, H. B. Liu, N. Chen, H. Q. Zhou, L. F. Sun, Y. J. Li and Y. L. Li, *Inorg Chem*, 2012, 51, 6771-6775.
- C. X. Ruan, J. Lou, D. D. Wang, C. Y. Zhang and W. Sun, *B Chem Soc Ethiopia*, 2011, 25, 443-450.
- F. Li, T. Kong, W. T. Bi, D. C. Li, Z. Li and X. T. Huang, *Appl Surf Sci*, 2009, 255, 6285-6289.
- J. Rodriguez-Moreno, E. Navarrete-Astorga, E. A. Dalchiele, R. Schreiber, J. R. Ramos-Barrado and F. Martin, *Chem Commun*, 2014, 50, 5652-5655.
- W. W. He, H. M. Jia, X. X. Li, Y. Lei, J. Li, H. X. Zhao, L. W. Mi, L. Z. Zhang and Z. Zheng, *Nanoscale*, 2012, 4, 3501-3506.
- X. L. Yu, C. B. Cao, H. S. Zhu, Q. S. Li, C. L. Liu and Q. H. Gong, *Adv Funct Mater*, 2007, 17, 1397-1401.
- P. Roy and S. K. Srivastava, *J Nanosci Nanotechno*, 2008, 8, 1523-1527.
- X. C. He, H. L. Shen, W. Wang, J. H. Pi, Y. Hao and X. B. Shi, *Appl Surf Sci*, 2013, 282, 765-769.
- Y. H. Ni, R. Liu, X. F. Cao, X. W. Wei and H. M. Hong, *Mater Lett*, 2007, 61, 1986-1989.
- M. Hromadova, M. Salmain, N. Fischer-Durand, L. Pospisil and G. Jaouen, *Langmuir*, 2006, 22, 506-511.
- S. Comby and T. Gunnlaugsson, *Acs Nano*, 2011, 5, 7184-7197.
- H. B. Noh, M. A. Rahman, J. E. Yang and Y. B. Shim, *Biosens Bioelectron*, 2011, 26, 4429-4435.
- D. P. Tang, R. Niessner and D. Knopp, *Biosens Bioelectron*, 2009, 24, 2125-2130.
- G. S. Lai, H. L. Zhang, T. Tamanna and A. M. Yu, *Anal Chem*, 2014, 86, 1789-1793.
- Z. Y. Zhong, M. X. Li, D. I. Xiang, N. Dai, Y. Qing, D. Wang and D. P. Tang, *Biosens Bioelectron*, 2009, 24, 2246-2249.
- C. Crosson and C. Rossi, *Biosens Bioelectron*, 2013, 42, 453-459.
- X. Cao, S. W. Liu, Q. C. Feng and N. Wang, *Biosens Bioelectron*, 2013, 49, 256-262.

ARTICLE

Detection of human immunoglobulin G by label-free electrochemical immunoassay modified with ultralong CuS nanowires

Cite this: DOI: 10.1039/x0xx00000x

Received 00th November 2014,
Accepted 00th November 2014

DOI: 10.1039/x0xx00000x

www.rsc.org/

Ning Wang^a, Caizhen Gao^{a, b}, Yu Han^{a, b}, Xiaomin Huang^{a, b}, Ying Xu^{a, b}, and Xia Cao^{b, c*}

^a School of Chemistry and Environment, Beijing University of Aeronautics and Astronautics, Beijing, 100191, China.

^b Beijing Institute of Nanoenergy and Nanosystems Chinese Academy of Science, Beijing, 100083, China.

^c School of Chemistry and Biological Engineering, University of Science and Technology Beijing, Beijing, 100083, China.

Table of contents entry:

A novel label-free electrochemical immunoassay modified with ultralong CuS nanowires was developed for the detection of human immunoglobulin G.

